Europe PMC Funders Group
Author Manuscript
Neuroimage. Author manuscript; available in PMC 2014 July 15.

Published in final edited form as:
Neuroimage. 2010 April 1; 50(2): 524–531. doi:10.1016/j.neuroimage.2009.12.058.

The test-retest reliability of 18F-DOPA PET in assessing striatal and extrastriatal presynaptic dopaminergic function

Alice Egerton[1,2,3], **Arsime Demjaha**[1,3], **Philip McGuire**[3], **Mitul A. Mehta**[#1,2,3], and **Oliver D. Howes**[#1,2,3]

[1]Psychiatric Imaging, Medical Research Council Clinical Sciences Centre, Imperial College London, Hammersmith Hospital, Du Cane Road, London W12 0NN, United Kingdom

[2]Division of Neurosciences & Mental Health, Imperial College London, United Kingdom

[3]Department of Psychological Medicine, Institute of Psychiatry, King's College London, London SE5 8AF, United Kingdom

[#] These authors contributed equally to this work.

Abstract

Brain presynaptic dopaminergic function can be assessed using 18F-DOPA positron emission tomography (PET). Regional 18F-DOPA utilization may be used to index dopaminergic abnormalities over time or dopaminergic response to treatment in clinical populations. Such studies require prior knowledge of the stability of the 18F-DOPA signal in the brain regions of interest. Test-retest reliability was examined in eight healthy volunteers who each received two 18F-DOPA PET scans, approximately two years apart. 18F-DOPA utilization (k_i^{cer}) was determined using graphical analysis relative to a reference tissue input (Patlak et al., 1983). Reproducibility (measured as the within-subjects variation) and reliability (measured as intraclass correlation coefficients, ICCs), of 18F-DOPA k_i^{cer} was assessed in the structural and functional subdivisions of the striatum and select extrastriatal brain regions. Voxel-based median ICC maps were used to visualize the distribution of 18F-DOPA k_i^{cer} reliability across the brain. The caudate and putamen, and associative and sensorimotor, striatal subdivisions showed good reliability across the two scan sessions with bilateral ICCs ranging from 0.681 to 0.944. Reliability was generally lower in extrastriatal regions, with bilateral ICCs ranging from 0.235 in the amygdala to 0.894 in the thalamus. These data confirm the utility of 18F-DOPA PET in assessing dopaminergic function in the striatum and select extrastriatal areas, but highlight the limitations in using this approach to measure dopaminergic function in low uptake extrastriatal brain areas. This information can be used to optimize the experimental design of future studies investigating changes in brain dopaminergic function with 18F-DOPA.

Keywords

Dopamine; Positron Emission Tomography; 18F-DOPA; Striatum; Reproducibility, Reliability; Schizophrenia; Parkinson's disease, longitudinal, extrastriatal

Address for Correspondence: Dr Alice Egerton, Neuroimaging P067, Department of Psychological Medicine, Institute of Psychiatry, King's College London, London SE5 8AF, United Kingdom. Alice.Egerton@iop.kcl.ac.uk ; Telephone: +44 (0)207 848 0879 ; Fax: +44 (0)207 848 0976.

Europe PMC Funders Author Manuscripts
Europe PMC Funders Author Manuscripts

Europe PMC Funders Author Manuscripts

Europe PMC Funders Author Manuscripts

Introduction

The radiolabeled amino acid 3,4-dihydroxy-6-[18F]fluoro-L-phenylalanine (18F-DOPA) in combination with positron emission tomography (PET) has been used for over 25 years to index dopaminergic function in the living human brain. As DOPA is the precursor of dopamine, the extent of accumulation of 18F-DOPA in the brain reflects the functional integrity of the presynaptic dopaminergic synthesis (Cumming et al., 1997), and indexes aromatic acid decarboxylase (AADC) activity. Many studies have used 18F-DOPA in combination with PET imaging to characterize abnormalities in dopaminergic transmission that occur in a number of CNS disorders, in particular schizophrenia (Howes et al., 2007), and Parkinson's disease (Brooks, 2003b; Brooks and Piccini, 2006; Heiss and Hilker, 2004).

Striatal 18F-DOPA uptake shows potential as a biomarker for pathogenesis and disease progression in Parkinson's disease (Brooks et al., 2003; Brooks, 2003a; Jokinen et al., 2009), and schizophrenia (Bose et al., 2008). Likewise, radiolabeled DOPA uptake may also provide a means for determining the effects of treatment on the underlying pathophysiology; for example uptake in the striatum is increased by dopamine replacement therapies in Parkinson's Disease (Nakamura et al., 2001; Piccini et al., 2005; Whone et al., 2003); and modulated by administration of dopamine D2 receptor antagonist antipsychotic compounds (Danielsen et al., 2001; Grunder et al., 2003; Tedroff et al., 1998; Torstenson et al., 1998; Vernaleken et al., 2006; Vernaleken et al., 2008).

However, it is important to know the reproducibility and reliability of 18F-DOPA imaging in healthy subjects, both to interpret existing studies and to design future longitudinal studies. Furthermore, improvements in scanner resolution have enabled striatal regions to be subdivided along anatomical or functional lines (Drevets et al., 2001; Martinez et al., 2003; Mawlawi et al., 2001), and whilst the reliability of this has been evaluated for imaging D2 receptors (Martinez et al., 2003) it has not been evaluated for 18F-DOPA imaging. Reproducibility and reliability is potentially even more of an issue in quantification of 18F-DOPA utilization in extrastriatal regions because the signal to noise ratio is lower (Moore et al., 2003). There are limited published data on reproducibility / reliability of 18F-DOPA imaging in the human striatum (Vingerhoets et al., 1994; Vingerhoets et al., 1996) and none for scanning intervals greater than 10 weeks or for extrastriatal regions.

The aim of this study was to determine the test – retest reliability and reproducibility of 18F-DOPA imaging in the commonly sampled subdivisions of the striatum, and extrastriatal regions in which alterations 18F-DOPA utilization have previously been investigated (Bruck et al., 2001; Kumakura et al., 2008; McGowan et al., 2004; Moore et al., 2008; Nozaki et al., 2009; Vernaleken et al., 2007). Both the reproducibility (within-subjects variation) and reliability (scaled here as the intraclass correlation coefficient (ICC)), are presented. A two year scan interval was used as this provides data to inform long-term clinical studies. Furthermore a measure that is reliable over this time period is likely to be at least as reliable over shorter periods where PET scanner drift and other methodological factors are less evident.

Europe PMC Funders Author Manuscripts

Europe PMC Funders Author Manuscripts

Methods

Participants

Test-retest data was obtained in eight young, healthy adults (mean age 23.6 ± 3.5 years, range 19-28 years, 5 male, 6 right handed) as part of an ongoing research project (Howes et al., 2009) approved by the South London and Maudsley / Institute of Psychiatry NHS Trust. The Administration of Radioactive Substances Advisory Committee (ARSAC) granted permission to administer 18F-DOPA. All subjects provided written consent to participate in the study. Exclusion criteria for all participants included pregnancy, contraindication to imaging, personal history of neurologic, psychiatric medical illness, alcohol or other drug abuse or dependency. Subjects underwent structural magnetic resonance imaging to exclude intracranial abnormalities. Urinary drug testing before each PET scan confirmed the absence of illicit drugs in all subjects.

PET data acquisition

Each subject received two 18F-DOPA PET scans, administered approximately two years apart (mean ± SD = 113.6 ± 16 weeks). PET imaging was performed on an ECAT/ EXACT3D: Siemens/CTI (Knoxville, Tennessee) PET tomograph (spatial resolution: 4.8 (0.2) mm; sensitivity: 69 cps/Bq/mL). High resolution images of the whole brain were reconstructed from 95 planes with a section spacing of 2.425 mm.

Subjects received carbidopa (150 mg) and entacapone (400 mg) orally 1 hour before imaging (Sawle et al., 1994). Administration of carbidopa and entacapone reduces the formation of radiolabeled 18F-DOPA metabolites(Cumming et al., 1993; Guttman et al., 1993), increasing the signal to noise ratio (Hoffman et al., 1992; Sawle et al., 1994). The 400mg dose of entacapone used increases the amount of 18F signal in the plasma accounted for by unmetabolized 18F-DOPA from approximately 21 to 55% (Sawle et al., 1994). Subjects were positioned with the orbitomeatal line parallel to the transaxial plane of the tomograph and head position was marked and monitored via laser crosshairs and a camera. Head movement was minimized by a molded head rest and straps. A 5-minute transmission image was obtained before radiotracer injection using a 150MBq cesium Cs 137 rotating point source to correct for attenuation and scatter.

Approximately 150 MBq of 18F-DOPA was administered by bolus intravenous injection 30 seconds after the start of the PET imaging. Emission data were acquired in list mode for 95 minutes, rebinned into 26 time-frames (comprising a 30-second background frame, four 60-second frames, three 120-second frames, three 180-second frames, and finally fifteen 300-second frames), and reconstructed using a 3-dimensional reprojection algorithm.

Image processing

To correct for head movement during the scan, nonattenuation corrected dynamic images were denoised using a level 2, order 64 Battle-Lemarie wavelet filter (Turkheimer et al., 1999), and individual frames were realigned to a single frame acquired 8 minutes after 18F-DOPA injection using a mutual information algorithm (Studholme et al., 1996). The transformation parameters were then applied to the corresponding attenuation-corrected

Europe PMC Funders Author Manuscripts

Europe PMC Funders Author Manuscripts

frames, and the realigned frames were combined to create a movement-corrected dynamic image (from 6 to 95 minutes following 18F-DOPA administration) for analysis.

In Montreal Neurologic Institute (MNI) space, standardized volumes of interest (VOI) were defined in the cerebellum (the reference region), and bilaterally in the caudate nucleus, putamen, nucleus accumbens, pallidum, substantia nigra, thalamus, hippocampus, amygdale, anterior and posterior cingulate cortex, medial frontal gyrus, anterior orbital cortex and corpus callosum (white matter), using a probabilistic atlas (Hammers et al., 2003). In addition, the limbic, associative, and sensorimotor subdivisions of the whole striatal VOI were delineated using previously described criteria (Martinez et al., 2003). An 18F-DOPA template was normalized together with the VOI map to each individual PET summation (add) image using the statistical parametric mapping suite SPM5 (http://www.fil.ion.ucl.ac.uk/spm/). This procedure allowed VOIs to be placed automatically on individual 18F-DOPA PET images without observer bias.

18F-DOPA utilization, relative to the cerebellar reference tissue (k_i^{cer} min^{-1}), was calculated for each VOI both uni- and bilaterally using graphical analysis, adapted for a reference tissue input function (Hartvig et al., 1991; Hoshi et al., 1993; Patlak and Blasberg, 1985).

Statistical analysis

Statistical analysis was performed using SPSS (Version 15.0). Results with $p<0.05$ were considered statistically significant and data are presented as mean ± SD. Unpaired Student's t-tests were used to test for differences in the injected dose and specific activity of the 18F-DOPA radioactivity injected between test (Scan1) and retest (Scan2) scans. Paired Student's t-tests were used to test for differences in regional k_i^{cer} values between the test and retest conditions. Significant regional differences in 18F-DOPA k_i^{cer} between the sampled VOI were determined using repeated measures analysis of variance (ANOVA).

Power calculations were performed using 'PS' software (Dupont and Plummer, Jr., 1990). Here, the regional percentage change in 18F-DOPA k_i^{cer} in a typical within-subjects or between-subjects experiment involving 15 subjects (or 15 subjects per group) was estimated using a probability (power) of 0.8 and an associated Type 1 error probability (α) of 0.05. For the within-subjects design, regional standard deviation (SD) in k_i^{cer} was calculated as the SD of the within-subject difference in k_i^{cer} across scanning sessions. For the between-subjects design, regional SD in k_i^{cer} was estimated as the mean of SD from the test scans and the SD of the retest scans.

Determination of reliability and reproducibility

We used two methods to estimate reliability of regional 18F-DOPA k_i^{cer}; ICC for average k_i^{cer} values sampled from volumes of interest (VOI), and an optimized voxel-level ICC analysis (Caceres et al., 2009). The first approach is traditionally used to estimate the test-retest reliability of a PET method. The use of the ICC maps has the advantage that reliability can be expressed relative to the whole brain for voxel-level analysis (Caceres et al., 2009).

In both cases, test-retest reliability was calculated using the third ICC defined by (Shrout and Fleiss, 1979), where:

Europe PMC Funders Author Manuscripts

Europe PMC Funders Author Manuscripts

$$ICC\,(3,1) = (BMS - EMS)\,/\,(BMS + (k-1)\,EMS)$$

where BMS and EMS are the subject and error sums of squares respectively and *k* is the number of repeated sessions. This model estimates the correlation between subject 18F-DOPA k_i^{cer} values between scan sessions using two-way ANOVA with random subject effects and fixed session effects. We selected this model over a oneway random model as the observations (regional k_i^{cer}) were ordered into two sessions (test or retest scan), and the two-way random model additionally accounts for systematic sources of variance associated with session effects (see McGraw and Wong, 1996). ICC values can range from −1 to +1. An ICC of −1 denotes no reliability, and negative ICC values imply that variation is greater within- than between-subjects. An ICC value of +1 denotes maximum reliability; the closer the ICC is to +1 the greater extent of the variance is due to between-subject than within-subject variation.

The VAR measure of test-retest reproducibility was calculated as the percentage test-retest difference:

$$VAR = (\text{retest value} - \text{test value})\,/0.5\,(\text{test value} + \text{retest value}) \times 100$$

Voxel-based reliability analysis

Reliability maps were created using the Reliability Toolbox for SPM (www.brainmap.co.uk) described in Caceres et al., (2009). Briefly, parametric maps representing 18F-DOPA k_i^{cer} were calculated for each scan by application of the cerebellar reference region and Patlak analysis. Using SPM5, individual 18F-DOPA add_images were spatially normalized to the 18F-DOPA template, and the normalization parameters were then applied to the coregistered 18F-DOPA k_i^{cer} parametric maps. Normalized parametric maps were spatially smoothed with a Gaussian kernel of 8mm (FWHM). The reliability of the whole brain and striatum was calculated as the median of the ICC distribution for voxels within the respective volumes.

Results

There was no significant difference between test and retest scans in either the amount of radioactivity injected (MBq mean ± SD: Scan 1: 147.3±6.6; Scan 2: 147.7±2.7; t_{14}=−0.16; p=0.876) or the specific activity of 18F-DOPA (MBq/μmol mean ± SD: Scan 1: 28.3±5.9; Scan 2: 26.6 ± 19.3; $t_{8.32}$ = 0.23; p = 0.821).

Standard reliability analysis

Structural and functional subdivisions of the striatum—The mean ± SD 18F-DOPA k_i^{cer} values obtained in striatal VOIs are presented in Table 1. In the structural subdivisions of the striatum – the caudate nucleus, putamen and nucleus accumbens- there were significant regional differences in k_i^{cer} values (F_2 = 79.8; p<0.001) and post-hoc tests confirmed that k_i^{cer} values were significantly higher in the putamen than nucleus accumbens and caudate nucleus (p<0.001), and that k_i^{cer} in the nucleus accumbens was significantly

Europe PMC Funders Author Manuscripts

Europe PMC Funders Author Manuscripts

higher than that in the caudate nucleus ($p<0.001$). There were no significant effects of side or test versus retest scan or two- or three-way interactions between region, side and scan.

In the functional subdivisions of the striatum – the associative, sensorimotor and limbic regions- there were also significant regional differences in k_i^{cer} ($F_2 = 19.1$ $p<0.001$). Post-hoc analysis confirmed that k_i^{cer} values were significantly lower in the associative subdivision compared to both the sensorimotor ($p=0.001$) and limbic ($p=0.009$) subdivisions. 18F-DOPA k_i^{cer} also varied according to side ($F_1=7.6$; $p=0.028$), due to higher k_i^{cer} values overall on the left side. Whilst there was no significant effect of test versus retest scan ($F_1 = 1.9$), we did detect significant region x scan and region x side x scan interactions. Post-hoc analysis showed that k_i^{cer} was significantly lower in the retest compared to test condition in the right limbic striatum ($t_7 = 2.9$; $p=0.022$); this effect also reached trend levels of significance when the limbic striatum was analyzed with left and right sides combined ($t_7 = 2.1$; $p=0.075$). There was no further significant effect of scan in any of the other striatal functional subdivisions when analyzed uni- or bilaterally.

The spread of 18F-DOPA k_i^{cer} values between subjects is also presented in Table 1. Inspection of the spread of data (%CV) shows that between subjects variation was lowest in the nucleus accumbens structural division and limbic functional division of the striatum.

Mean percent test-retest differences and ranges of difference for k_i^{cer} values in the striatal structural and functional subdivisions are presented in Table 2. In all striatal divisions, reproducibility of 18F-DOPA k_i^{cer} was excellent (<10% VAR) and repeated measures ANOVA showed there was no significant difference in reproducibility of k_i^{cer} values obtained in the functional or structural subregions ($F_5=1.6$; $p=0.195$). Paired samples t-tests showed that there was no significant difference in the test-retest reproducibility in k_i^{cer} measures in any of the striatal subregions compared to the striatum as a whole ($t_7<1.7$; $p>0.13$).

Table 2 also presents the test-retest reliability values (ICCs) in striatal VOIs. In all striatal divisions except the limbic striatum and nucleus accumbens, reliability was good suggesting that measurement variance reflected between-subjects differences. In the nucleus accumbens, test-retest reliability was poor when examined unilaterally, less than 0.6 in both cases. This was somewhat improved when ICC values in this region were calculated with left and right sides combined (ICC = 0.738). In the limbic striatal functional subdivision, ICC values were particularly poor on the right side, (-0.381), but were higher on the left (0.755). The negative ICC value on the right side is indicative of greater within than between subjects variability, and reflects the significant difference in right limbic k_i^{cer} between the test and retest conditions (see above). For comparison, ICC values obtained using a one-way random model (ICC(1,1), Shrout and Fleiss, 1979), which does not account for session effects, were very similar to the ICC(3,1) values reported and gave a similar regional pattern of effects (data not shown).

Extrastriatal regions—Table 3 presents the mean k_i^{cer} values and spread of data that were obtained in extrastriatal VOI and white matter (corpus callosum). As expected, k_i^{cer} values in all extrastriatal regions were significantly lower (~10-50%) than those in the

striatum ($p<0.001$), but displayed regional differences ($F_8=172.0$ $p<0.001$). The rank order of k_i^{cer} values was pallidum = nigra > amygdala > hippocampus > anterior cingulate > thalamus = anterior orbital gyrus = medial frontal gyrus > posterior cingulate. Of the extrastriatal regions assessed, k_i^{cer} values in the pallidum, nigra, amygdala, hippocampus and anterior cingulate cortex were significantly greater than those in white matter (corpus callosum; $p = 0.038$ to < 0.001). However, k_i^{cer} values in the thalamus and anterior orbital gyrus did not differ from those in white matter ($p > 0.05$), whilst those in the medial frontal gyrus and posterior cingulate cortex were significantly lower than white matter values ($p = 0.043$ and $p < 0.001$ respectively). T-tests (uncorrected for multiple comparisons) showed a significant difference between k_i^{cer} values in the test and retest conditions in the bilateral pallidum ($t_7=2.6$; $p=0.037$); anterior cingulate cortex (bilateral $t_7=2.8$; $p=0.029$; right $t_7=2.7$; $p=0.031$); posterior cingulate cortex (bilateral $_{t7}=4.2$; $p=0.004$; right $_{t7}=4.2$; $p=0.004$; left $_{t7}=2.9$; $p=0.022$), right medial frontal gyrus ($_{t7}=5.7$; $p<0.001$) and also in white matter ($_{t7}=4.5$; $p=0.003$). In all instances, this was due to lower k_i^{cer} values in the retest compared to test condition.

The between subjects variation in extrastriatal regions was generally larger than that in striatal regions, with the largest variations (mean CV>15%) occurring in the substantia nigra, medial frontal and anterior orbital gyrus, and posterior cingulate cortex.

There was no significant difference in test-retest reproducibility (VAR) between the extrastriatal regions sampled ($F_8=1.739$; $p=0.109$). Test-retest variability in the pallidum ($t_7 = -3.4$; $p=0.011$), posterior cingulate cortex ($t_7 = -2.7$; $p=0.030$) and anterior orbital gyrus ($t_7 = -2.4$; $p=0.049$) were significantly greater than that in the striatum, and there was a similar trend in the medial frontal gyrus ($t_7=-2.2$; $p=0.067$). VAR in white matter was no different from that in the extrastriatal regions sampled ($p > 0.999$).

Test-retest reliability was generally moderate or poor (ICC <0.7) in extrastriatal VOI, although ICC values were generally higher when left and right sides were combined than when they were measured in each hemisphere separately. The pallidum, substantia nigra, thalamus, anterior and posterior cingulate and anterior orbital cortex, showed bilateral ICC values >0.6, whilst reliability was poorer (ICC <0.6) in the hippocampus, amygdala and medial frontal gyrus. Analysis of k_i^{cer} values extracted from white matter gave ICC values of 0.78.

Power analysis

The results of the power analysis for within- and between-subjects study designs are presented in Table 5. This shows that for within subject studies the smallest detectable changes in k_i^{cer} are in the order of ~3-6% in striatal regions, and from 4% to 15% in extrastriatal regions. If a between-subjects design is used, the smallest detectable differences in k_i^{cer} are in the order of 7-11% in the striatum and 7-18% in extrastriatal regions.

Voxel-based reliability analysis

Figure 1 illustrates the voxel-wise reliability for the 18F-DOPA parametric images across the whole brain. The median ICC computed from the whole brain is 0.22 (standard error

Europe PMC Funders Author Manuscripts
Europe PMC Funders Author Manuscripts

Europe PMC Funders Author Manuscripts

Europe PMC Funders Author Manuscripts

(SE) = 0.067) and the striatum is 0.65 (SE = 0.047). The figure shows that the reliability is highest in the striatum with less consistent regional effects outside of this area. This is exemplified by the amygdala (median ICC = 0.37, SE = 0.105) and pallidum (median ICC = 0.36, SE = 0.068), both of which show higher reliability than the whole brain but considerably lower reliability than the striatum.

Figure 2 shows the distribution of median ICC values. In comparison to distribution across the whole brain, the distribution of striatal ICC values is skewed towards high ICC values. Thus, the probability of any one voxel being of high reliability in the striatum is greater than that in the whole brain.

Discussion

In this study we show that 18F-DOPA k_i^{cer} measures have good reproducibility and reliability in the striatum over two years. The voxel-level ICC maps clearly showed that the most reliable voxels were clustered together within the striatum, resulting in a distribution of ICCs with a median value much higher than the whole brain. As expected, the reliability and reproducibility of 18F-DOPA k_i^{cer} measures in extrastriatal regions was generally poorer. These findings indicate that 18F-DOPA imaging can be reliably used to study disease progression and treatment effects in long-term clinical studies in the striatum and to a lesser degree in select extrastriatal areas.

The reliability of striatal subdivisions

In all striatal regions sampled in the VOI analysis, the within-subjects variability was low (<10%). As variability was similar when assessed according to either the structural or functional subdivisions of the striatum, these data show that application of the functional subdivision model of the striatum does not result in a loss of measurement reproducibility. The low within-subjects variation in the more dorsal regions of the striatum (putamen, caudate nucleus, sensorimotor striatum and associative striatum) was associated with good reliability of 18F-DOPA k_i^{cer}.

In the ventral aspects of the striatum (nucleus accumbens and limbic striatum VOI), reliability was somewhat poorer, and in the limbic striatum on the right side, there was a significant decrease in 18F-DOPA k_i^{cer} in the retest compared to test condition. The small size of these VOIs means that they are particularly susceptible to motion artifacts, and the effect of these may be exacerbated by proximity to both low- and high-uptake adjacent structures. Therefore, even small amounts of head movement may markedly influence the amount of activity measured in the ventral striatum (Mawlawi et al., 2001). Whilst we corrected for head movement during the scans, realignment is limited and unable to correct for movements that occur within frames. Application of alternative movement correction technologies, such as head motion tracking, may improve reliability in future studies (Montgomery et al., 2006). In addition, quantitation of the ventral striatum may suffer from registration errors, due to deviations in individual anatomy. Resolution constraints also mean that small ROI volumes, such as those of the ventral striatum, are particularly susceptible to underestimation of radioactivity concentrations due to partial volume and spill-over effects

Europe PMC Funders Author Manuscripts

Europe PMC Funders Author Manuscripts

(Mawlawi et al., 2001). One limitation of the present study is that we did not correct for partial volume effects, the influence of which could be examined in future studies.

The reliability of extrastriatal regions

In extrastriatal regions the relatively low reliability and the larger range of difference in k_i^{cer} probably reflects the low signal-to-noise ratio in these areas. The general improvement in ICC scores in all regions when data from left and right hemispheres was combined is probably due to an increase in signal-to-noise ratio when the number of voxels is increased (Hirvonen et al., 2003). The reliability and reproducibility of 18F-DOPA k_i^{cer} measures in some extrastriatal regions was poor, with bilateral ICCs < 0.5 in the hippocampus, amygdala and medial frontal gyrus, and bilateral %VAR > 15% in the posterior cingulate cortex and medial frontal gyrus. Reproducibility and reliability were moderate (ICC > 0.6 %VAR ≤~10 bilaterally) in the substantia nigra, thalamus, pallidum, anterior cingulate cortex and anterior orbital cortex.

In the thalamus, posterior cingulate cortex, anterior orbital gyrus and medial frontal gyrus, k_i^{cer} values were equal to or less than that in adjacent white matter. Higher 18F-DOPA k_i^{cer} values in white matter than cortical grey matter regions have also recently been reported by (Cropley et al., 2008). As stated in Cropley et al., (2008), higher 18F-DOPA k_i^{cer} values in white over grey matter are unreasonable as AADC is minimally present in white matter. This has lead to questions of the validity of Patlak reference tissue analysis in low uptake, extrastriatal VOI (Cropley et al., 2008), and the suggestion that partial volume correction for white matter should be applied in these regions (Cropley et al., 2008). Therefore, although the thalamus and anterior orbital cortex showed moderate reproducibility and reliability, the similarity of k_i^{cer} values in these regions to those unreasonably obtained in white matter suggests that measurement in these regions may be invalid. Overall, we conclude that assessment of 18F-DOPA utilization using the cerebellar reference tissue approach, and without partial volume correction, may be valid and have acceptable reproducibility in the substantia nigra, pallidum and anterior cingulate cortex, but is highly questionable in other extrastriatal areas.

The use of 18F-DOPA for measuring dopamine synthesis in the striatum is well established, and striatal 18F-DOPA uptake positively correlates with postmortem levels of striatal dopamine (Snow et al., 1993). The relationship between 18F-DOPA utilization and dopamine synthesis in extrastriatal regions is less clear. In addition to converting DOPA to dopamine, AADC also converts 5-hydroxytryptophan to serotonin (Bouchard et al., 1981) and contributes to the production of trace amines such as tyramine and tryptamine (see Lindemann and Hoener, 2005)). Therefore the degree to which 18F-DOPA uptake reflects dopamine synthesis capacity in extrastriatal regions is unclear.

Implications of our findings

Power analysis clearly indicated that smaller percent changes in k_i^{cer} are detectable in all regions using a within-subjects experimental design, due to the lower variability in k_i^{cer} within- than between-subjects. Using a within-subjects design in 15 subjects, which is typical and practicable for longitudinal imaging studies of this type, the present data

Europe PMC Funders Author Manuscripts

Europe PMC Funders Author Manuscripts

estimate that there is sufficient power to estimate true changes in k_i^{cer} of 3-6% in striatal regions. Our findings also indicate that measurement of k_i^{cer} in select extrastriatal regions shows acceptable reliability, but that measurements in many extrastriatal regions are likely to be unreliable.

The high reliability in the striatum supports the use of 18F-DOPA imaging as a diagnostic test for CNS disorders such as Parkinson's disease and schizophrenia (Bose et al., 2008; Eshuis et al., 2009). Furthermore it indicates that 18F-DOPA imaging could be used clinically to guide treatment, for example to identify patients whose dopaminergic system shows limited response to first-line treatment, or fast disease progression, and may therefore benefit from an early switch to second-line therapies.

The relatively long time period between test and retest scans (approximately 2 years) means that variation in k_i^{cer} may arise from both methodological and biological factors. Over this time period, there was no change in 18F-DOPA radiosynthesis, and both the amount and specific activity of 18F-DOPA injected did not differ between test and retest scans. We were not aware of any change in scanner performance, and all images were processed using the same methodology (at the same time). Whilst DOPA utilization or storage may decline with age (Kumakura et al., 2008; Ota et al., 2006), we would not expect to see any significant decline over a two year period in healthy young adults. There was no change in mental or physical health status of any of the subjects included in this study over the scanning period.

Conclusions

In conclusion, 18F-DOPA imaging provides a reliable measure of dopaminergic function in the striatum, and acceptable reliability in select striatal subdivisions and extrastriatal areas. These findings show it is feasible to study clinically significant changes in dopaminergic function in striatal and select extrastriatal regions using 18F-DOPA imaging.

Acknowledgments

This research was supported by the Medical Research Council, UK.

Reference List

Bose SK, Turkheimer FE, Howes OD, Mehta MA, Cunliffe R, Stokes PR, Grasby PM. Classification of schizophrenic patients and healthy controls using [18F] fluorodopa PET imaging. Schizophr.Res. 2008; 106:148–155. [PubMed: 18849151]

Bouchard S, Bousquet C, Roberge AG. Characteristics of dihydroxyphenylalanine/5-hydroxytryptophan decarboxylase activity in brain and liver of cat. J.Neurochem. 1981; 37:781–787. [PubMed: 6974228]

Brooks DJ. Imaging end points for monitoring neuroprotection in Parkinson's disease. Ann.Neurol. 2003a; 53(Suppl 3):S110–S118. [PubMed: 12666103]

Brooks DJ. PET studies on the function of dopamine in health and Parkinson's disease. Ann.N.Y.Acad.Sci. 2003b; 991:22–35. [PubMed: 12846971]

Brooks DJ, Frey KA, Marek KL, Oakes D, Paty D, Prentice R, Shults CW, Stoessl AJ. Assessment of neuroimaging techniques as biomarkers of the progression of Parkinson's disease. Exp.Neurol. 2003; 184(Suppl 1):S68–S79. [PubMed: 14597329]

Brooks DJ, Piccini P. Imaging in Parkinson's disease: the role of monoamines in behavior. Biol.Psychiatry. 2006; 59:908–918. [PubMed: 16581032]

Europe PMC Funders Author Manuscripts

Bruck A, Portin R, Lindell A, Laihinen A, Bergman J, Haaparanta M, Solin O, Rinne JO. Positron emission tomography shows that impaired frontal lobe functioning in Parkinson's disease is related to dopaminergic hypofunction in the caudate nucleus. Neurosci.Lett. 2001; 311:81–84. [PubMed: 11567783]

Caceres A, Hall DL, Zelaya FO, Williams SC, Mehta MA. Measuring fMRI reliability with the intra-class correlation coefficient. Neuroimage. 2009; 45:758–768. [PubMed: 19166942]

Cropley VL, Fujita M, Bara-Jimenez W, Brown AK, Zhang XY, Sangare J, Herscovitch P, Pike VW, Hallett M, Nathan PJ, Innis RB. Pre- and post-synaptic dopamine imaging and its relation with frontostriatal cognitive function in Parkinson disease: PET studies with [11C]NNC 112 and [18F]FDOPA. Psychiatry Res. 2008; 163:171–182. [PubMed: 18504119]

Cumming P, Deep P, Rousset O, Evans A, Gjedde A. On the rate of decarboxylation of dopa to dopamine in the living mammillian brain. Ann.N.Y.Acad.Sci. 1997; 835:274–308. [PubMed: 9616781]

Cumming P, Leger GC, Kuwabara H, Gjedde A. Pharmacokinetics of plasma 6-[18F]fluoro-L-3,4-dihydroxyphenylalanine ([18F]Fdopa) in humans. J.Cereb.Blood Flow Metab. 1993; 13:668–675. [PubMed: 8314919]

Danielsen EH, Smith D, Hermansen F, Gjedde A, Cumming P. Acute neuroleptic stimulates DOPA decarboxylase in porcine brain in vivo. Synapse. 2001; 41:172–175. [PubMed: 11400183]

Drevets WC, Gautier C, Price JC, Kupfer DJ, Kinahan PE, Grace AA, Price JL, Mathis CA. Amphetamine-induced dopamine release in human ventral striatum correlates with euphoria. Biol.Psychiatry. 2001; 49:81–96. [PubMed: 11164755]

Dupont WD, Plummer WD Jr. Power and sample size calculations. A review and computer program. Control Clin.Trials. 1990; 11:116–128. [PubMed: 2161310]

Eshuis SA, Jager PL, Maguire RP, Jonkman S, Dierckx RA, Leenders KL. Direct comparison of FP-CIT SPECT and F-DOPA PET in patients with Parkinson's disease and healthy controls. Eur.J.Nucl Med.Mol.Imaging. 2009; 36:454–462. [PubMed: 19037637]

Grunder G, Vernaleken I, Muller MJ, Davids E, Heydari N, Buchholz HG, Bartenstein P, Munk OL, Stoeter P, Wong DF, Gjedde A, Cumming P. Subchronic haloperidol downregulates dopamine synthesis capacity in the brain of schizophrenic patients in vivo. Neuropsychopharmacology. 2003; 28:787–794. [PubMed: 12655326]

Guttman M, Leger G, Reches A, Evans A, Kuwabara H, Cedarbaum JM, Gjedde A. Administration of the new COMT inhibitor OR-611 increases striatal uptake of fluorodopa. Mov Disord. 1993; 8:298–304. [PubMed: 8341294]

Hammers A, Allom R, Koepp MJ, Free SL, Myers R, Lemieux L, Mitchell TN, Brooks DJ, Duncan JS. Three-dimensional maximum probability atlas of the human brain, with particular reference to the temporal lobe. Hum.Brain Mapp. 2003; 19:224–247. [PubMed: 12874777]

Hartvig P, Agren H, Reibring L, Tedroff J, Bjurling P, Kihlberg T, Langstrom B. Brain kinetics of L-[beta-11C]dopa in humans studied by positron emission tomography. J.Neural Transm.Gen.Sect. 1991; 86:25–41. [PubMed: 1751027]

Heiss WD, Hilker R. The sensitivity of 18-fluorodopa positron emission tomography and magnetic resonance imaging in Parkinson's disease. Eur.J.Neurol. 2004; 11:5–12. [PubMed: 14692881]

Hirvonen J, Aalto S, Lumme V, Nagren K, Kajander J, Vilkman H, Hagelberg N, Oikonen V, Hietala J. Measurement of striatal and thalamic dopamine D2 receptor binding with 11C-raclopride. Nucl.Med.Commun. 2003; 24:1207–1214. [PubMed: 14627846]

Hoffman JM, Melega WP, Hawk TC, Grafton SC, Luxen A, Mahoney DK, Barrio JR, Huang SC, Mazziotta JC, Phelps ME. The effects of carbidopa administration on 6-[18F]fluoro-L-dopa kinetics in positron emission tomography. J.Nucl.Med. 1992; 33:1472–1477. [PubMed: 1634937]

Hoshi H, Kuwabara H, Leger G, Cumming P, Guttman M, Gjedde A. 6-[18F]fluoro-L-dopa metabolism in living human brain: a comparison of six analytical methods. J.Cereb.Blood Flow Metab. 1993; 13:57–69. [PubMed: 8417011]

Howes OD, Montgomery AJ, Asselin MC, Murray RM, Grasby PM, McGuire PK. Molecular imaging studies of the striatal dopaminergic system in psychosis and predictions for the prodromal phase of psychosis. Br J Psychiatry Suppl. 2007; 51:s13–s18. [PubMed: 18055930]

Europe PMC Funders Author Manuscripts

Howes OD, Montgomery AJ, Asselin MC, Murray RM, Valli I, Tabraham P, Bramon-Bosch E, Valmaggia L, Johns L, Broome M, McGuire PK, Grasby PM. Elevated striatal dopamine function linked to prodromal signs of schizophrenia. Arch.Gen.Psychiatry. 2009; 66:13–20. [PubMed: 19124684]

Jokinen P, Helenius H, Rauhala E, Bruck A, Eskola O, Rinne JO. Simple ratio analysis of 18F-fluorodopa uptake in striatal subregions separates patients with early Parkinson disease from healthy controls. J.Nucl Med. 2009; 50:893–899. [PubMed: 19443601]

Kumakura Y, Vernaleken I, Buchholz HG, Borghammer P, Danielsen E, Grunder G, Heinz A, Bartenstein P, Cumming P. Age-dependent decline of steady state dopamine storage capacity of human brain: An FDOPA PET study. Neurobiol.Aging. 2008

Lindemann L, Hoener MC. A renaissance in trace amines inspired by a novel GPCR family. Trends Pharmacol.Sci. 2005; 26:274–281. [PubMed: 15860375]

Martinez D, Slifstein M, Broft A, Mawlawi O, Hwang DR, Huang Y, Cooper T, Kegeles L, Zarahn E, Abi-Dargham A, Haber SN, Laruelle M. Imaging human mesolimbic dopamine transmission with positron emission tomography. Part II: amphetamine-induced dopamine release in the functional subdivisions of the striatum. J.Cereb.Blood Flow Metab. 2003; 23:285–300. [PubMed: 12621304]

Mawlawi O, Martinez D, Slifstein M, Broft A, Chatterjee R, Hwang DR, Huang Y, Simpson N, Ngo K, Van Heertum R, Laruelle M. Imaging human mesolimbic dopamine transmission with positron emission tomography: I. Accuracy and precision of D(2) receptor parameter measurements in ventral striatum. J Cereb.Blood Flow Metab. 2001; 21:1034–1057. [PubMed: 11524609]

McGowan S, Lawrence AD, Sales T, Quested D, Grasby P. Presynaptic dopaminergic dysfunction in schizophrenia: a positron emission tomographic [18F]fluorodopa study. Arch.Gen.Psychiatry. 2004; 61:134–142. [PubMed: 14757589]

McGraw KO, Wong SP. Forming inferences about some intraclass correlation coefficients. Psychological Methods. 1996; 1:30–46.

Montgomery AJ, Thielemans K, Mehta MA, Turkheimer F, Mustafovic S, Grasby PM. Correction of head movement on PET studies: comparison of methods. J.Nucl.Med. 2006; 47:1936–1944. [PubMed: 17138736]

Moore RY, Whone AL, Brooks DJ. Extrastriatal monoamine neuron function in Parkinson's disease: an 18F-dopa PET study. Neurobiol.Dis. 2008; 29:381–390. [PubMed: 18226536]

Moore RY, Whone AL, McGowan S, Brooks DJ. Monoamine neuron innervation of the normal human brain: an 18F-DOPA PET study. Brain Res. 2003; 982:137–145. [PubMed: 12915249]

Nakamura T, Dhawan V, Chaly T, Fukuda M, Ma Y, Breeze R, Greene P, Fahn S, Freed C, Eidelberg D. Blinded positron emission tomography study of dopamine cell implantation for Parkinson's disease. Ann.Neurol. 2001; 50:181–187. [PubMed: 11506400]

Nozaki S, Kato M, Takano H, Ito H, Takahashi H, Arakawa R, Okumura M, Fujimura Y, Matsumoto R, Ota M, Takano A, Otsuka A, Yasuno F, Okubo Y, Kashima H, Suhara T. Regional dopamine synthesis in patients with schizophrenia using L-[beta-11C]DOPA PET. Schizophr.Res. 2009; 108:78–84. [PubMed: 19056247]

Ota M, Yasuno F, Ito H, Seki C, Nozaki S, Asada T, Suhara T. Age-related decline of dopamine synthesis in the living human brain measured by positron emission tomography with L-[beta-11C]DOPA. Life Sci. 2006; 79:730–736. [PubMed: 16580023]

Patlak CS, Blasberg RG. Graphical evaluation of blood-to-brain transfer constants from multiple-time uptake data. Generalizations. J Cereb.Blood Flow Metab. 1985; 5:584–590. [PubMed: 4055928]

Patlak CS, Blasberg RG, Fenstermacher JD. Graphical evaluation of blood-to-brain transfer constants from multiple-time uptake data. J.Cereb.Blood Flow Metab. 1983; 3:1–7. [PubMed: 6822610]

Piccini P, Pavese N, Hagell P, Reimer J, Bjorklund A, Oertel WH, Quinn NP, Brooks DJ, Lindvall O. Factors affecting the clinical outcome after neural transplantation in Parkinson's disease. Brain. 2005; 128:2977–2986. [PubMed: 16246865]

Sawle GV, Burn DJ, Morrish PK, Lammertsma AA, Snow BJ, Luthra S, Osman S, Brooks DJ. The effect of entacapone (OR-611) on brain [18F]-6-L-fluorodopa metabolism: implications for levodopa therapy of Parkinson's disease. Neurology. 1994; 44:1292–1297. [PubMed: 8035933]

Shrout PE, Fleiss JL. Intraclass correlations: uses in assessing rater reliability. Psychol.Bull. 1979; 86:420–428. [PubMed: 18839484]

Europe PMC Funders Author Manuscripts

Snow BJ, Tooyama I, McGeer EG, Yamada T, Calne DB, Takahashi H, Kimura H. Human positron emission tomographic [18F]fluorodopa studies correlate with dopamine cell counts and levels. Ann.Neurol. 1993; 34:324–330. [PubMed: 8363349]

Studholme C, Hill DL, Hawkes DJ. Automated 3-D registration of MR and CT images of the head. Med.Image Anal. 1996; 1:163–175. [PubMed: 9873927]

Tedroff J, Torstenson R, Hartvig P, Sonesson C, Waters N, Carlsson A, Neu H, Fasth KJ, Langstrom B. Effects of the substituted (S)-3-phenylpiperidine (-)-OSU6162 on PET measurements in subhuman primates: evidence for tone-dependent normalization of striatal dopaminergic activity. Synapse. 1998; 28:280–287. [PubMed: 9517836]

Torstenson R, Hartvig P, Langstrom B, Bastami S, Antoni G, Tedroff J. Effect of apomorphine infusion on dopamine synthesis rate relates to dopaminergic tone. Neuropharmacology. 1998; 37:989–995. [PubMed: 9833628]

Turkheimer FE, Brett M, Visvikis D, Cunningham VJ. Multiresolution analysis of emission tomography images in the wavelet domain. J Cereb.Blood Flow Metab. 1999; 19:1189–1208. [PubMed: 10566965]

Vernaleken I, Buchholz HG, Kumakura Y, Siessmeier T, Stoeter P, Bartenstein P, Cumming P, Grunder G. 'Prefrontal' cognitive performance of healthy subjects positively correlates with cerebral FDOPA influx: an exploratory [18F]-fluoro-L-DOPA-PET investigation. Hum.Brain Mapp. 2007; 28:931–939. [PubMed: 17133402]

Vernaleken I, Kumakura Y, Buchholz HG, Siessmeier T, Hilgers RD, Bartenstein P, Cumming P, Grunder G. Baseline [(18)F]-FDOPA kinetics are predictive of haloperidol-induced changes in dopamine turnover and cognitive performance: A positron emission tomography study in healthy subjects. Neuroimage. 2008; 40:1222–1231. [PubMed: 18262797]

Vernaleken I, Kumakura Y, Cumming P, Buchholz HG, Siessmeier T, Stoeter P, Muller MJ, Bartenstein P, Grunder G. Modulation of [18F]fluorodopa (FDOPA) kinetics in the brain of healthy volunteers after acute haloperidol challenge. Neuroimage. 2006; 30:1332–1339. [PubMed: 16439159]

Vingerhoets FJ, Schulzer M, Ruth TJ, Holden JE, Snow BJ. Reproducibility and discriminating ability of fluorine-18-6-fluoro-L-Dopa PET in Parkinson's disease. J.Nucl Med. 1996; 37:421–426. [PubMed: 8772636]

Vingerhoets FJ, Snow BJ, Schulzer M, Morrison S, Ruth TJ, Holden JE, Cooper S, Calne DB. Reproducibility of fluorine-18-6-fluorodopa positron emission tomography in normal human subjects. J.Nucl Med. 1994; 35:18–24. [PubMed: 8285951]

Whone AL, Watts RL, Stoessl AJ, Davis M, Reske S, Nahmias C, Lang AE, Rascol O, Ribeiro MJ, Remy P, Poewe WH, Hauser RA, Brooks DJ. Slower progression of Parkinson's disease with ropinirole versus levodopa: The REAL-PET study. Ann.Neurol. 2003; 54:93–101. [PubMed: 12838524]

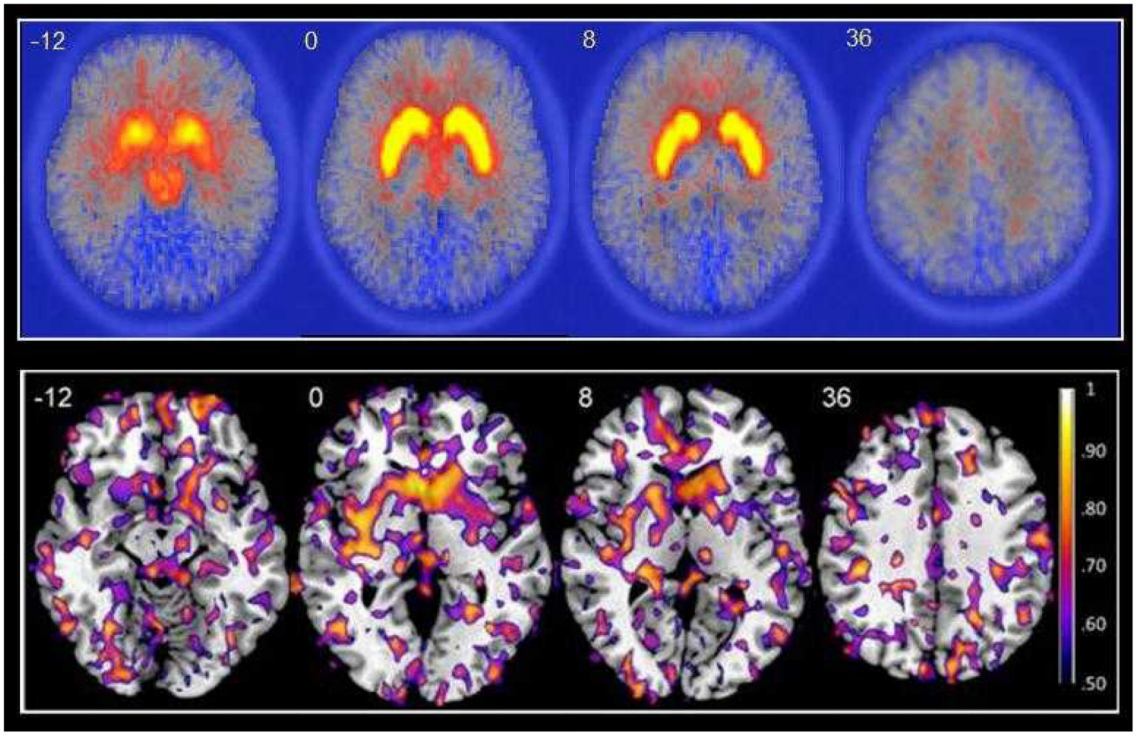

Figure 1.

Top panel: Mean parametric 18F-DOPA k_i^{cer} maps for eight healthy volunteers during the first (test) scanning session. Four representative transaxial slices at z=--12, z=0, z=8 and z=36 are overlaid on an 18F-DOPA template. The high k_i^{cer} values (yellow areas) obtained in the striatum are clearly visible. Bottom panel: ICC maps of 18F-DOPA k_i^{cer} for eight healthy volunteers scanned over two sessions. Four representative transaxial slices at z=--12, z=0, z=8 and z=36 show ICC values greater than 0.50 overlaid on the high resolution single subject T1-weighted MRI image in MNI space. The highest reliability (yellow areas) is clearly visible in the large clusters of the striatum.

Europe PMC Funders Author Manuscripts
Europe PMC Funders Author Manuscripts

Europe PMC Funders Author Manuscripts

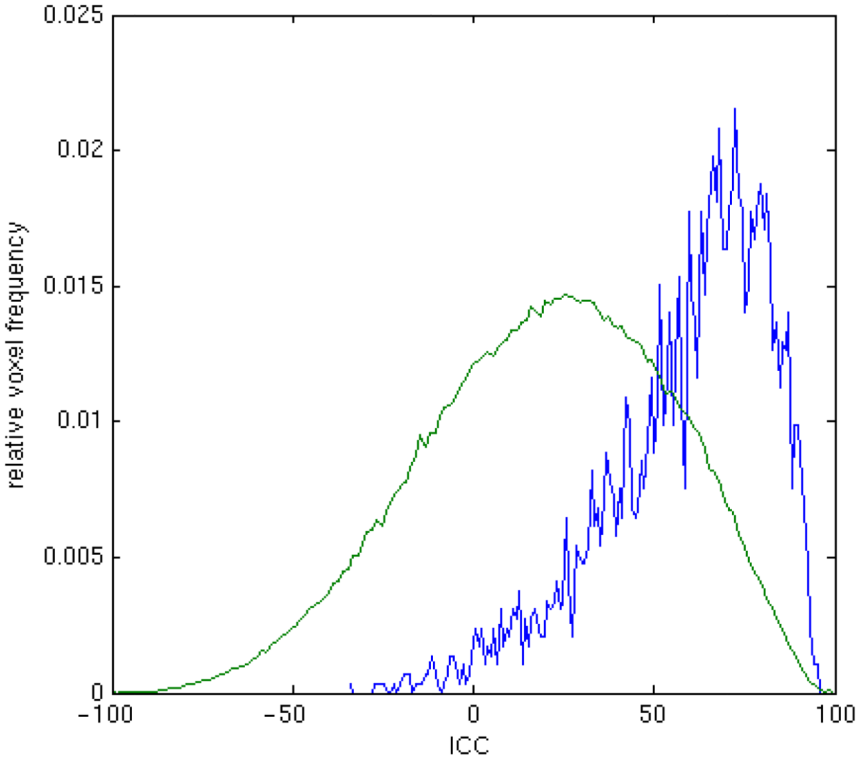

Figure 2.

The figure shows the distribution of median ICC values across voxels in the striatum (blue) and whole brain (green). The skewed distribution of ICC values in striatal voxels compared to the whole brain is clearly visible.

Europe PMC Funders Author Manuscripts

Europe PMC Funders Author Manuscripts

Europe PMC Funders Author Manuscripts

Table 1

Between-subjects variation in 18F-DOPA k_i^{cer} in striatal subdivisions. 18F-DOPA k_i^{cer} values acquired during test and retest scans in 8 subjects are presented as mean±S.D. min^{-1}. Spread or variation between subjects is expressed as percentage coefficient of variation (%CV) = SD/mean ×100.

	Test		Retest	
	k_i^{cer} (mean±SD)	**CV (%)**	**k_i^{cer} (mean±SD)**	**CV (%)**
Whole striatum	0.01417±0.00127	8.9%	0.01381±0.00127	9.2%
Left	0.01427±0.00120	8.4%	0.01408±0.00135	9.6%
Right	0.01409±0.00135	9.6%	0.01354±0.00132	9.7%
Associative	0.01368±0.00130	9.5%	0.01331±0.00137	10.3%
Left	0.01361±0.00130	9.5%	0.01350±0.00150	11.1%
Right	0.01375±0.00138	10.1%	0.01314±0.00142	10.8%
Sensorimotor	0.01485±0.00159	10.7%	0.01489±0.00127	8.5%
Left	0.01473±0.00141	9.5%	0.01512±0.00116	7.7%
Right	0.01489±0.00178	12.0%	0.01458±0.00155	10.7%
Limbic	0.01491±0.00085	5.7%	0.01408±0.00120	8.5%
Left	0.01540±0.00106	6.9%	0.01443±0.00157	10.9%
Right	0.01435±0.00095	6.6%	0.01369±0.00088*	6.4%
Caudate nucleus	0.01203±0.00120	10.0%	0.01195±0.00131	10.9%
Left	0.01181±0.00118	12.2%	0.01205±0.00132	11.0%
Right	0.01224±0.00120	9.0%	0.01186±0.00139	11.7%
Putamen	0.01522±0.00134	8.8%	0.01512±0.00142	9.4%
Left	0.01541±0.00119	7.7%	0.01530±0.00137	10.4%
Right	0.01503±0.00164	10.9%	0.01493±0.00156	9.0%
Nucleus accumbens	0.01317±0.00090	6.5%	0.01313±0.00101	7.7%
Left	0.01311±0.00103	7.9%	0.01308±0.00111	8.5%
Right	0.01334±0.00124	9.3%	0.01320±0.00124	9.4%

* $p<0.05$ test versus retest scan.

Europe PMC Funders Author Manuscripts

Europe PMC Funders Author Manuscripts

Table 2

Striatal 18F-DOPA k_i^{cer} test-retest characteristics, shown as estimates of absolute variability (% VAR), range of difference in VAR, and reliability (intraclass correlation coefficient, ICC).

	% VAR (mean±S.D.)	Range of difference	ICC
Whole striatum	4.50 ± 3.59	1.29 - 11.65	0.843
Left	3.95 ± 2.23	2.05 - 8.88	0.878
Right	6.08 ± 4.92	0.45 – 14.38	0.759
Associative	4.04 ± 2.84	0.19 – 9.74	0.886
Left	3.83 ± 1.53	1.95 - 6.83	0.914
Right	5.91± 5.19	0.14 – 13.56	0.823
Sensorimotor	5.89 ± 4.82	0.90 – 13.08	0.681
Left	6.30 ± 3.86	2.02 – 13.42	0.659
Right	5.30 ± 4.96	0.09 – 13.02	0.800
Limbic	7.20 ± 6.50	0.39 – 16.99	0.427
Left	6.89 ± 6.58	0.28 – 18.08	0.755
Right	8.95 ± 7.12	1.25 – 22.64	-0.381
Caudate nucleus	2.97 ± 2.06	0.59 – 6.77	0.944
Left	4.21 ± 1.49	1.97 – 6.10	0.932
Right	5.23 ± 5.63	0.17 – 14.75	0.792
Putamen	4.52 ± 3.15	1.25 – 10.65	0.824
Left	5.16 ± 4.15	0.71 – 13.24	0.702
Right	4.26 ± 3.67	0.08 – 8.03	0.859
Nucleus Accumbens	4.52 ± 2.33	2.18 – 8.25	0.738
Left	6.39 ± 5.52	0.88 – 16.18	0.410
Right	7.72 ± 4.60	3.35 – 16.36	0.501

Europe PMC Funders Author Manuscripts

Europe PMC Funders Author Manuscripts

Table 3

Between-subjects variation in 18F-DOPA k_i^{cer} values in extrastriatal brain regions. 18F-DOPA k_i^{cer} values acquired during test and retest scan are presented as mean±S.D. min^{-1}. Spread or variation between subjects is expressed as percentage coefficient of variation (%CV) = SD/mean ×100.

	Test		Retest	
	k_i^{cer} (mean±SD)	CV (%)	k_i^{cer} (mean±SD)	CV (%)
White matter	0.00264 ± 0.00023	8.9%	0.00239 ± 0.00024*	9.9%
Pallidum	0.00772 ± 0.00078	10.1%	0.00713 ± 0.00072*	10.1%
Left	0.00549 ± 0.00093	16.9%	0.00494 ± 0.00049	10.0%
Right	0.01010 ± 0.00078	8.3%	0.00929 ± 0.00112	12.1%
Substantia nigra	0.00744 ± 0.00160	19.1%	0.00734 ± 0.00100	13.7%
Left	0.00832 ± 0.00144	17.4%	0.00805 ± 0.00135	16.8%
Right	0.00664 ± 0.00160	24.1%	0.00675 ± 0.00127	18.8%
Thalamus	0.00258 ± 0.00024	9.4%	0.00249 ± 0.00033	13.4%
Left	0.00248 ± 0.00031	12.7%	0.00241 ± 0.00042	17.4%
Right	0.00268 ± 0.00029	10.9%	0.00256 ± 0.00035	13.6%
Hippocampus	0.00394 ± 0.00035	8.8%	0.00375 ± 0.00047	12.4%
Left	0.00396 ± 0.00039	9.8%	0.00374 ± 0.00034	9.0%
Right	0.00388 ± 0.00041	10.5%	0.00399 ± 0.00027	6.8%
Amygdala	0.00607 ± 0.00042	6.9%	0.00575 ± 0.00042	7.2%
Left	0.00602 ± 0.00046	7.7%	0.00561 ± 0.00047	8.5%
Right	0.00610 ± 0.00056	9.1%	0.00590 ± 0.00038	6.5%
Anterior cingulate	0.00316 ± 0.00026	8.4%	0.00290 ± 0.00035*	12.0%
Left	0.00318 ± 0.00031	9.8%	0.00299 ± 0.00032	10.5%
Right	0.00316 ± 0.00026	8.2%	0.00281 ± 0.00041*	14.7%
Posterior cingulate	0.00183 ± 0.00028	15.3%	0.00153 ± 0.00025*	16.3%
Left	0.00168 ± 0.00027	16.0%	0.00140 ± 0.00028*	20.2%
Right	0.00197 ± 0.00033	17.0%	0.00163 ± 0.00027*	16.4%
Medial frontal gyrus	0.00198 ± 0.00040	20.1%	0.00193 ± 0.00028	14.5%
Left	0.00207 ± 0.00036	17.9%	0.00199 ± 0.00033	16.5%
Right	0.00207 ± 0.0024	14.7%	0.00187 ± 0.00025*	13.2%
Anterior orbital gyrus	0.00225 ± 0.00035	15.7%	0.00224 ± 0.00040	17.8%
Left	0.00226 ± 0.00040	17.9%	0.00231 ± 0.00047	20.4%
Right	0.00224 ± 0.00033	14.7%	0.00217 ± 0.00035	16.2%

Europe PMC Funders Author Manuscripts

Europe PMC Funders Author Manuscripts

Table 4

Extrastriatal 18F-DOPA k_i^{cer} test-retest characteristics, shown as estimates of absolute variability (% VAR), range of difference in VAR, and reliability (intraclass correlation coefficient, ICC).

	% VAR (mean±S.D.)	Range of difference	ICC
White matter	10.53 ± 5.1	2.01 – 16.34	0.778
Pallidum	10.76 ± 4.30	4.49 – 16.47	0.624
Left	13.67 ± 10.41	0.88 – 27.87	0.454
Right	11.06 ± 8.84	1.04 – 24.76	0.465
Substantia nigra	10.48 ± 8.52	1.47 – 23.35	0.646
Left	14.87 ± 10.22	0.45 – 34.28	0.436
Right	15.28 ± 8.82	4.29 – 29.38	0.614
Thalamus	5.64 ± 3.23	0.32 – 11.93	0.894
Left	12.01 ± 6.94	2.02 – 22.68	0.598
Right	6.34 ± 8.92	0.32 – 27.64	0.686
Hippocampus	9.21 ± 10.16	1.90 – 32.82	0.459
Left	10.67 ± 9.17	0.39 – 26.24	−0.077
Right	10.37 ± 3.72	4.12 – 15.18	0.170
Amygdala	6.96 ± 7.22	0.39 – 20.79	0.235
Left	10.94 ± 6.58	2.83 – 24.51	0.017
Right	7.36 ± 6.77	0.53 – 16.90	0.290
Anterior cingulate	9.48 ± 8.97	0.46 – 23.73	0.609
Left	8.69 ± 5.42	2.59 – 16.56	0.645
Right	12.58 ± 13.22	0.52 – 34.33	0.454
Posterior cingulate	17.91 ± 11.42	4.36 – 30.51	0.708
Left	20.31 ± 13.27	2.20 – 39.59	0.536
Right	18.55 ± 11.68	2.86 – 35.98	0.714
Medial frontal gyrus	16.66 ± 14.03	1.22 – 45.69	0.401
Left	10.41 ± 6.06	4.01 – 39.88	0.221
Right	17.99 ± 13.22	2.51 – 21.41	0.917
Anterior orbital cortex	10.83 ± 6.72	0.02 – 17.69	0.704
Left	16.03 ± 7.00	6.14 – 25.59	0.552
Right	8.93 ± 6.00	2.78 – 21.26	0.779

Europe PMC Funders Author Manuscripts

Europe PMC Funders Author Manuscripts

Table 5

Regional detectable percentage changes in k_i^{cer} for within- and between-subjects experimental designs as estimated using power analysis

The regional detectable % changes in k_i^{cer} (%Δ k_i^{cer}) are shown for a within-subjects design in 15 subjects, and a between-subjects design with 15 subjects per group, with power=0.8 and α=0.05. The within- and between-subjects standard deviations (SD) used in the analysis are also presented.

	Within-subjects design		Between-subjects design	
	SD	%Δ k_i^{cer}	SD	%Δ k_i^{cer}
Whole Striatum	0.000712	4.0	0.001270	9.5
Associative striatum	0.000641	3.3	0.001339	10.4
Sensorimotor striatum	0.001147	6.0	0.001427	10.2
Limbic striatum	0.001117	6.0	0.001029	7.3
Caudate nucleus	0.000420	2.7	0.001253	11.0
Putamen	0.000821	4.2	0.001382	9.6
Nucleus accumbens	0.000679	4.0	0.000935	7.5
Pallidum	0.000651	6.8	0.000750	10.3
Substantia nigra	0.001034	10.9	0.001211	17.3
Thalamus	0.000135	4.1	0.000288	11.8
Hippocampus	0.000427	8.6	0.000406	10.9
Amygdala	0.000515	6.8	0.000416	7.3
Anterior cingulate	0.000274	7.0	0.000306	10.2
Posterior cingulate	0.000202	9.4	0.000264	15.3
Medial frontal gyrus	0.000376	14.9	0.000338	18.1
Anterior orbital gyrus	0.000290	10.1	0.000376	17.7